Supporting Information

Hybrid hollow spheres of carbon@$Co_xNi_{1-x}MoO_4$ as advanced electrode for high-performance asymmetric supercapacitor

Junsheng Lin[a], Lei Yao[a], Zheling Li[b], Peixin Zhang[a], Wenhua Zhong[a], Qiuhua Yuan[a], and Libo Deng[a*]

[a]College of Chemistry and Environmental Engineering, Shenzhen University, Shenzhen 518060, China

[b]National Graphene Institute and School of Materials, University of Manchester, Manchester, M13 9PL, UK

[*] Corresponding author: Denglb@szu.edu.cn; Tel: +86-755-26536157

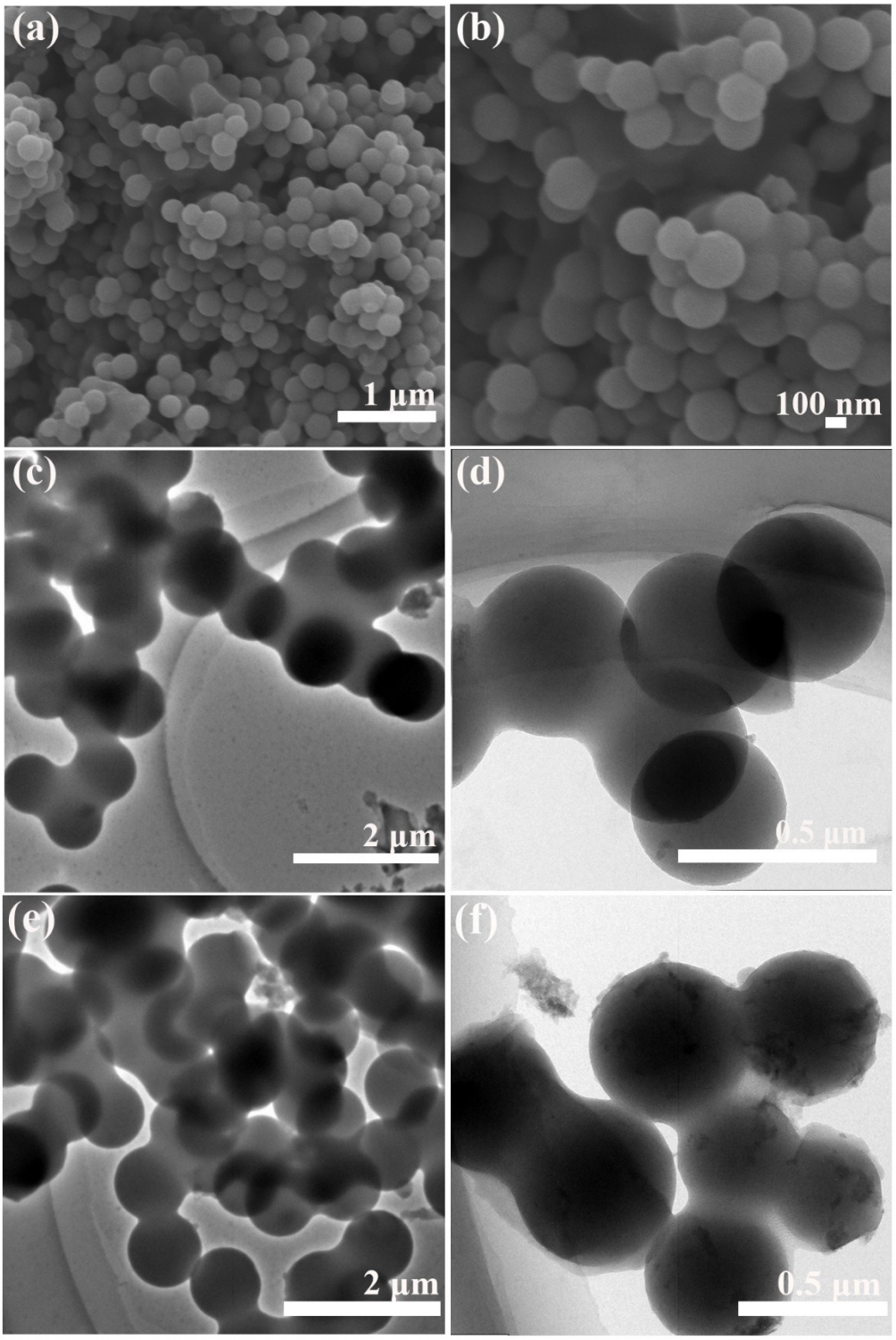

Figure S1 (a and b) SEM images of CNS, and TEM images of CNS (c and d) and PCNS (e and f)

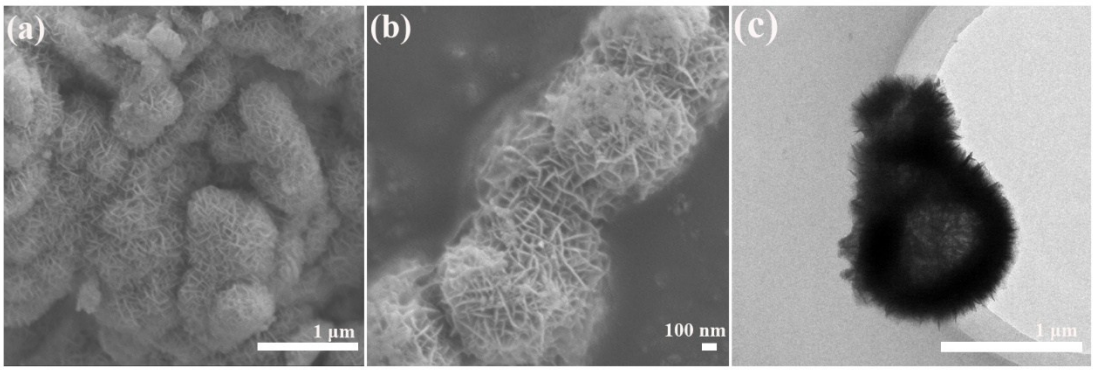

Figure S2 (a and b) SEM images of pure $NiMoO_4$, and (c) TEM images of PCNS@$NiMoO_4$.

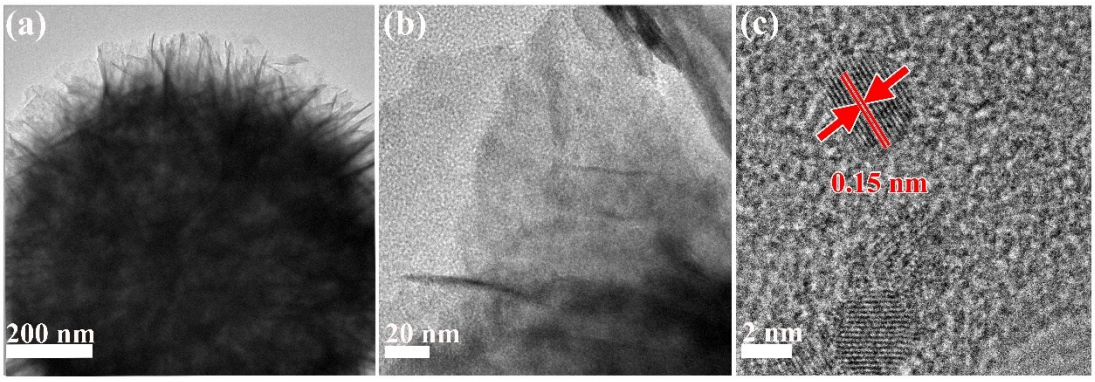

Figure S3 TEM images of PCNS@$Co_{0.21}Ni_{0.79}MoO_4$ (a, b and c).

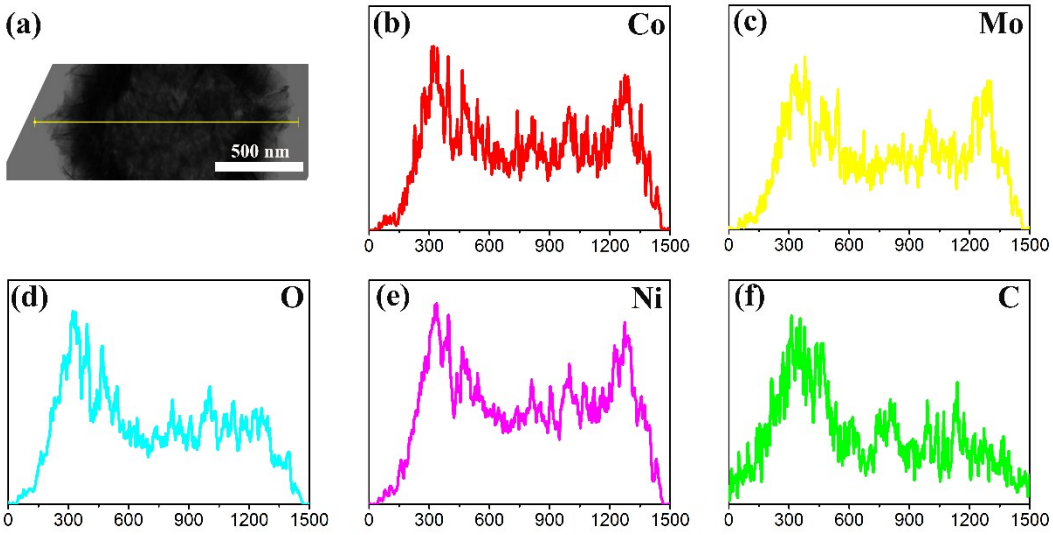

Figure S4 (a) HAADF images of PCNS@$Co_{0.21}Ni_{0.79}MoO_4$ and Element line spectrum of (b) Co, (c) Mo, (d) O, (e) Ni and (f) C

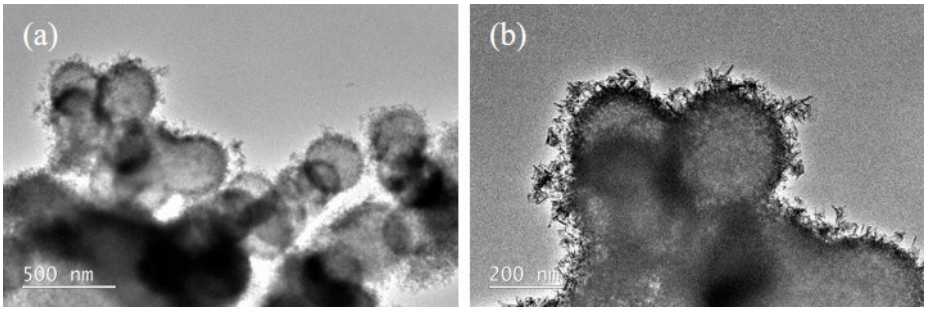

Figure S5 TEM images for PCNS@MnO_2.

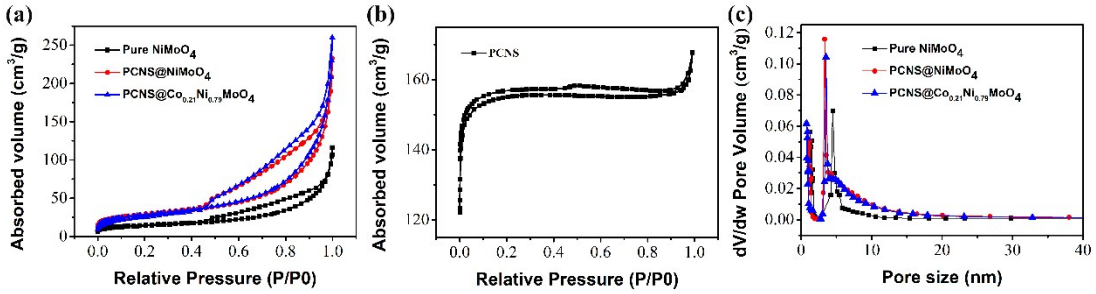

Figure S6 (a) N_2 adsorption and desorption isotherms of pure $NiMoO_4$, PCNS@$NiMoO_4$ and PCNS@$Co_{0.21}Ni_{0.79}MoO_4$, (b) N_2 adsorption and desorption isotherms of PCNS, (c) BJH pore-size distribution of pure $NiMoO_4$, PCNS@$NiMoO_4$ and PCNS@$Co_{0.21}Ni_{0.79}MoO_4$.

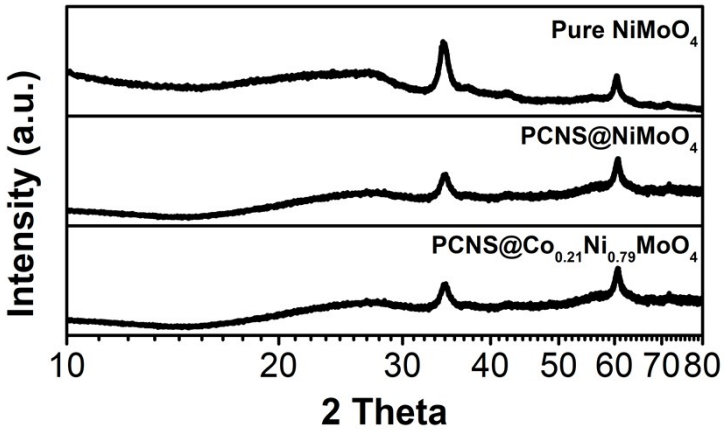

Figure S7 XRD patterns of Pure $NiMoO_4$, PCNS@$NiMoO_4$, PCNS@$Co_{0.21}Ni_{0.79}MoO_4$.

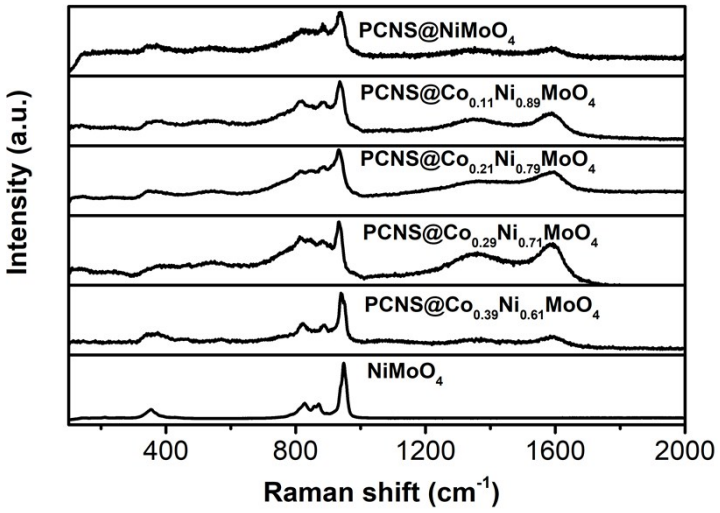

Figure S8 Raman spectra of all the samples.

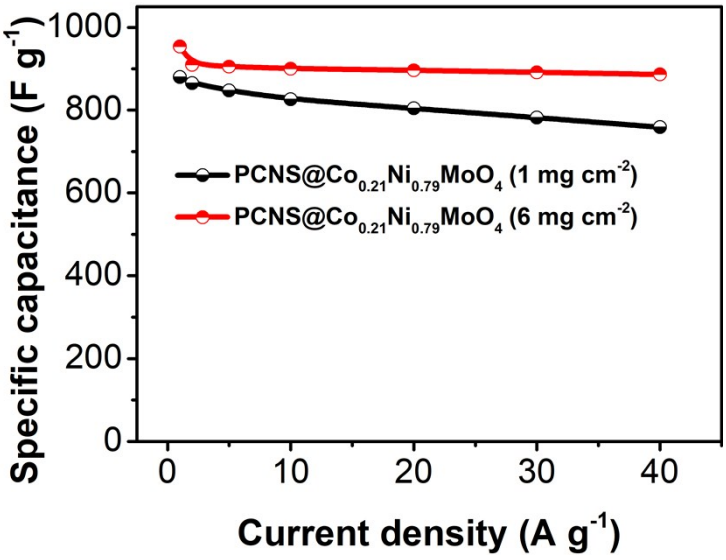

Figure S9 Rate performance the PCNS@$Co_{0.21}Ni_{0.79}MoO_4$ electrode with mass loadings of 1 and 6 mg cm^{-2}.

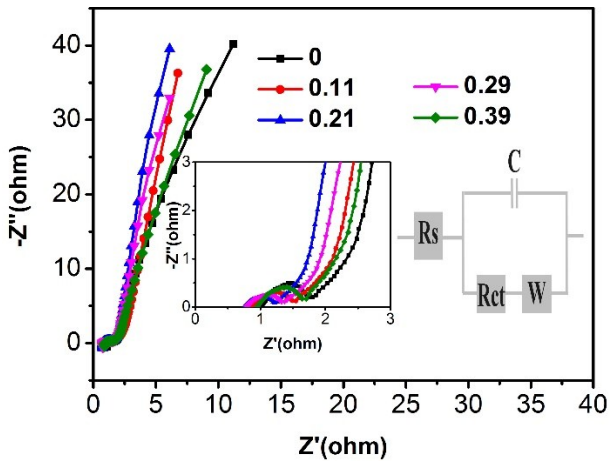

Figure S10 Nyquist plots in the frequency range from 0.1 Hz to 100 kHz of the electrodes with different compositions.

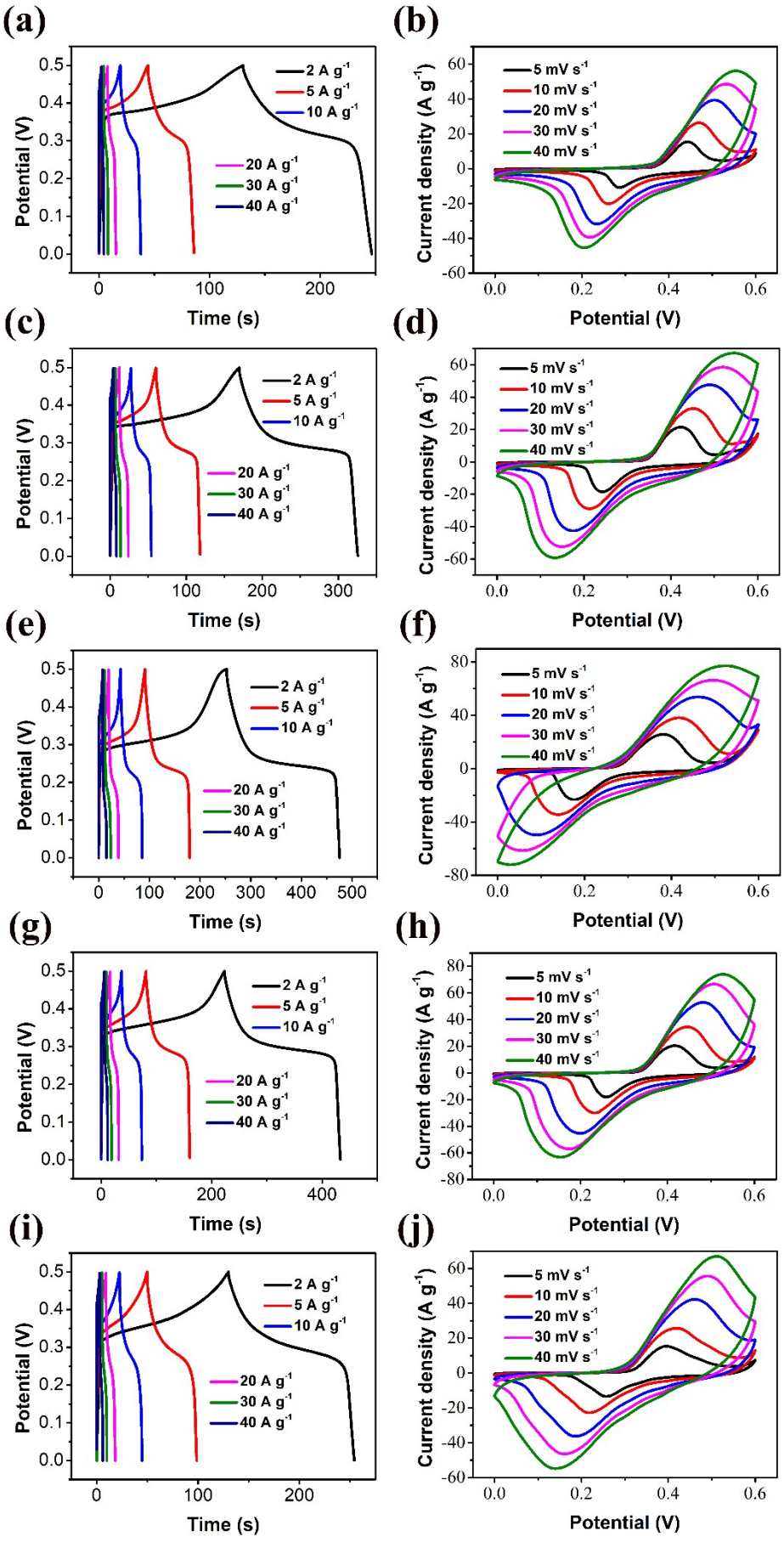
(a)
Potential (V)
Time (s)
2 A g-1
5 A g-1
10 A g-1
20 A g-1
30 A g-1
40 A g-1
(b)
Current density (A g-1)
Potential (V)
5 mV s-1
10 mV s-1
20 mV s-1
30 mV s-1
40 mV s-1
(c)
(d)
(e)
(f)
(g)
(h)
(i)
(j)

Figure S11 GCD and CV curves of (a and b) $NiMoO_4$, (c and d) $Co_{0.11}Ni_{0.89}MoO_4$, (e and f) $Co_{0.21}Ni_{0.79}MoO_4$, (g and h) $Co_{0.29}Ni_{0.71}MoO_4$, and (i and j) $Co_{0.39}Ni_{0.61}MoO_4$.

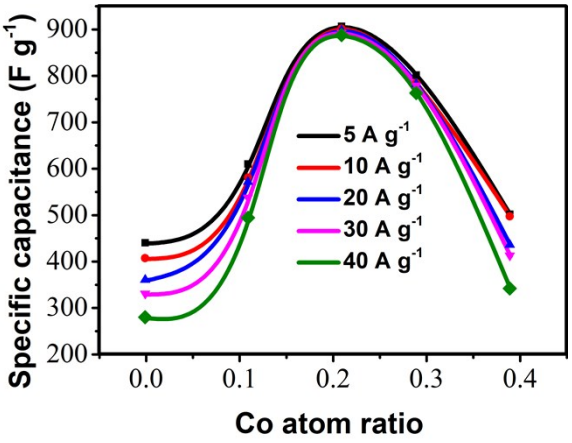

Figure S12 The specific capacitances of PCNS@$Co_xNi_{1-x}MoO_4$ electrodes at different current densities as a function of the Co content.

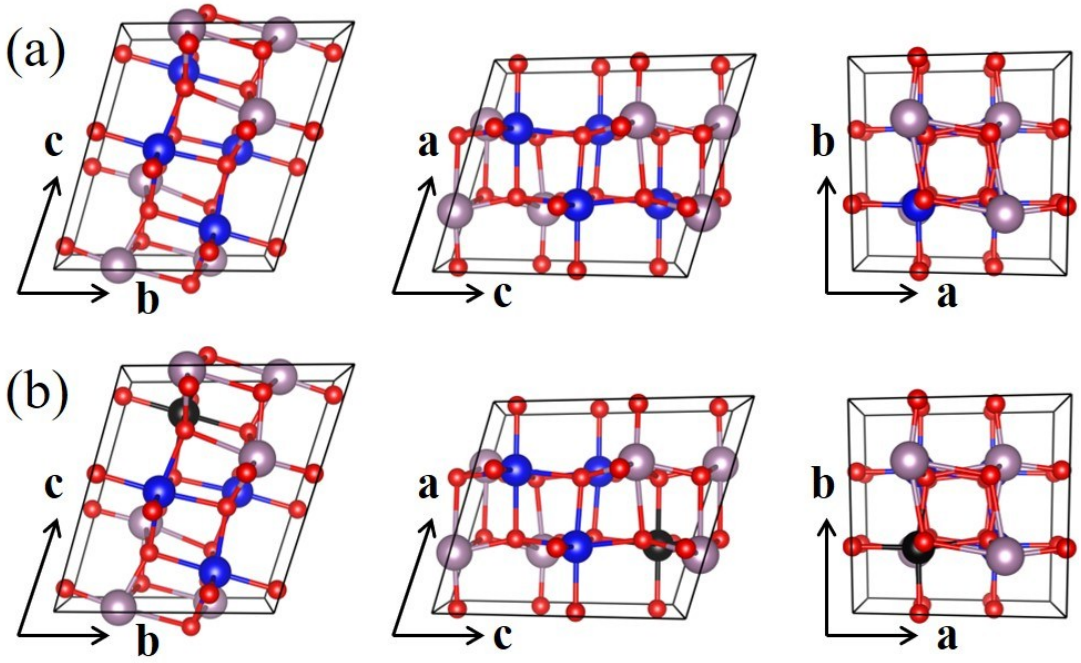

Figure S13 Schematic structure model of (a) $NiMoO_4$ and (b) $Co_{0.25}Ni_{0.75}MoO_4$. Black, blue, grey and red balls represent Co, Ni, Mo and O atoms, respectively.

Table S1 Calculated lattice constants and band gaps of $NiMoO_4$ and $Co_{0.25}Ni_{0.75}MoO_4$.

System	Lattice constants (Å)	Gap (eV)

	|a|	|b|	|c|	Spin majority	Spin minority
$NiMoO_4$	6.528	6.528	7.740	3.56	3.43
$Co_{0.25}Ni_{0.75}MoO_4$	6.535	6.535	7.754	3.80	3.05

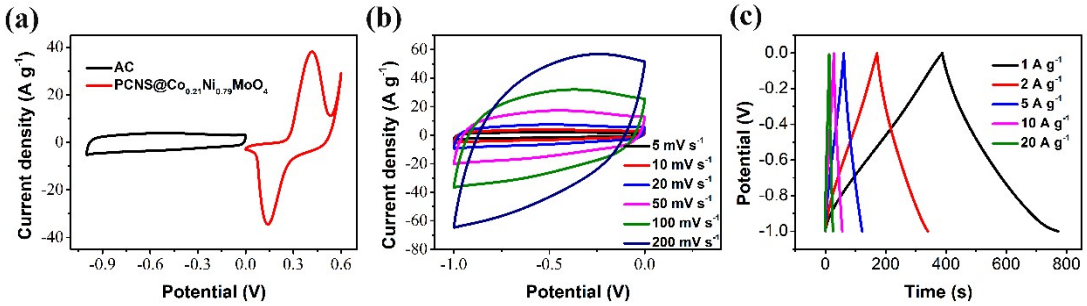

Figure S14 (a) CV curve of AC and PCNS@$Co_{0.21}Ni_{0.79}MoO_4$ at 10 mV s^{-1}, (b and c) CV and GCD curves of AC.